Valorisation of an aromatic compound from a renewable natural resource: eugenol, by hemi-synthesis of new molecules for antimicrobial and anticorrosion applications

BAHIJA REBBAH

rebbahbahia@gmail.com

Sultan Moulay Slimane University

Abderrahim El haib

Sultan Moulay Slimane University

Sara Lahmady

Beni Mellal

Yassine Aallam

Sulan Moulay Slimane University, FST

Wissal Kotmani

Beni Mellal

Rachid Hnini

Sultan Moulay Slimane University

Maryse Gouygou

CNRS, Universty of toulouse, UPS, Toulouse-INP

Issam Forsal

Beni Mellal

ElMostapha Rakib

Sultan Moulay Slimane University

Abdellah Hannioui

Sultan Moulay Slimane University

Research Article

Keywords: Natural Product, Eugenol, Heterocyclic Compounds, Microbiology, and Corrosion activity

Posted Date: December 2nd, 2024

DOI: https://doi.org/10.21203/rs.3.rs-5415548/v1

Additional Declarations: No competing interests reported.

Valorisation of an aromatic compound from a renewable natural resource: eugenol, by hemi-synthesis of new molecules for antimicrobial and anticorrosion applications

Bahija Rebbah[1*], Abderrahim El haib[2*], Sara Lahmady[3], Yassine Aallam[4], Wissal Kotmani[3], Rachid Hnini[5], Maryse Gouygou[6], Issam Forsal[3], ElMostapha Rakib[1] and Abdellah Hannioui[1].

[1] Moleculare, Chemistry, Materials and Catalysis, Laboratory, Faculty of Science and Technology Sultan Moulay Slimane University, B.P. 523. Beni Mellal. Mrocco. hannioui@yahoo.fr
[2] Chemical Processes and Applied Materials Laboratory, Polydisciplinary Faculty, Sultan Moulay Slimane University, PB:592, Beni Mellal, Morocco. elhaibabderrahim@gmail.com
[3] Laboratory of Engineering and Applied Technologies, School of Technology, Beni Mellal, Morocco. forsalissam@yahoo.fr
[4] Laboratory of Biological Engineering, Pathology, and Functional Biology Team, Sulan Moulay Slimane University, FST, PO. Box : 23000 Beni Mellal, Morocco.Yassine.aallam@gmail.com
[5] Laboratory of Biological Engineering, Pathology and Functional Biology Team, Sultan Moulay Slimane University, FST, Beni Mellal, Morocco. rachid.hnini@hotmail.com
[6] CNRS, Coordination Chemistry Laboratory, Universty of toulouse, UPS, Toulouse-INP, 205 Narbonne road, BP 44099, F-31077 Toulouse Cedex 4 france. maryse.gouygou@lcc-toulouse.fr
*Correspondence: rebbahbahia@gmail; Tel: +212 606750890. elhaibabderrahim@gmail.com; Tel: +212 699109850.

Abstract: Various semi-synthetic derivatives of eugenol have been reported in recent years with improved bioactivities and a broad mode of action. The main objective of this work is to develop new heterocyclic and acyclic molecules with potential biological and electrochemical activities from a readily available natural product, eugenol, known chemically as 4-allyl-2-methoxyphenol with the molecular formula $C_{10}H_{12}O_2$. It belongs to a class of natural phenolic monoterpenoids. Here we describe the synthesis of eugenol derivatives and the evaluation of their biological and electrochemical activities. These new eugenol derivatives were synthesized and characterized by NMR and FTIR. Electrochemical methods, such as polarisation curves and electrochemical impedance spectroscopy, were used to evaluate the corrosion inhibition properties of eugenol. Regarding corrosion inhibition properties, eugenol derivatives have shown that they can be used as organic corrosion inhibitors in aggressive environments to reduce the corrosion process of metals in industry. According to the results obtained in this work, several products tested showed significant efficacy against various pathogenic bacteria studied, particularly at concentrations of 100 µg/mL. Most of them synthesized showed a zone of inhibition greater than 11 mm.
Keywords: Natural Product, Eugenol, Heterocyclic Compounds, Microbiology, and Corrosion activity.

1. Introduction

People have been using plants in phytotherapy, pharmacology, and agri-food for centuries, thanks to their properties discovered by chance. Nature's biodiversity offers researchers infinite research opportunities, particularly in the discovery of molecules with interesting chemical and biological properties, whether therapeutic, phytosanitary, or industrial. Nature's impressive richness, complexity, and beauty are often a source of inspiration for researchers.

To develop new products based on a natural product with high added value in the biological [1] and electrochemical fields [2, 3] we turned our attention to eugenol, the main constituent of clove essential oil. Chemically known as 2-methoxy-4(2-propenyl)phenol, eugenol has outstanding olfactory and biological properties and pharmacological activities such as antioxidant, antiviral anti-inflammatory, anticancer, antiviral, antidiabetic, antiparasitic, antimicrobial [4, 5, 6, 7, 8, 9, 10] and others.

Molecular modification of the structures of naturally occurring biologically active substances is one of the main strategies for enhancing healthy biological effects and reducing potential side effects. The valorization of these natural substances involves their functionalization, to enhance the recognized biological activity of the natural molecule or discover new activities.

Various semi-synthetic derivatives of eugenol with different acyclic and heterocyclic rings have been reported in recent years, with improved bioactivities and a broad mode of action [11, 12, 13, 14].

Despite advances in the synthesis of antimicrobial drugs, microbial infections remain a threat to humanity [15]. Increased resistance of pathogenic microbial strains to antimicrobial drugs leads to ineffective treatment and persistent infections, sometimes resulting in death [16]. It is therefore necessary to develop powerful new antimicrobial agents for the treatment of resistant pathogenic microbial strains.

Corrosion is a degradation of materials due to chemical or electrochemical reactions with the external environment, resulting in a progressive loss of materials at the interface with this environment. The impact of corrosion is widespread in various industrial sectors, and its economic cost is higher [2,3]. HCl is one of the most widely used acids in industrial applications, precipitating the degradation of metal substrates by electrochemical and chemical means. Countermeasures against corrosion in this environment include metal coatings, anodic and cathodic protection, galvanizing, and the deployment of corrosion inhibitors [17]. In acidic environments, the use of inhibitors is a superior strategy for protecting metallic materials.

In the present study (Figure 1), and as part of our ongoing efforts in the field of hemi-synthesis of new compounds derived from natural products [18, 19, 3], we have synthesized new eugenol-derived hybrid compounds **2, 3,** and **3a-3f** combining acyclic or heterocyclic units, via atom-economy reactions, a project which falls within the context of green chemistry and sustainable development.

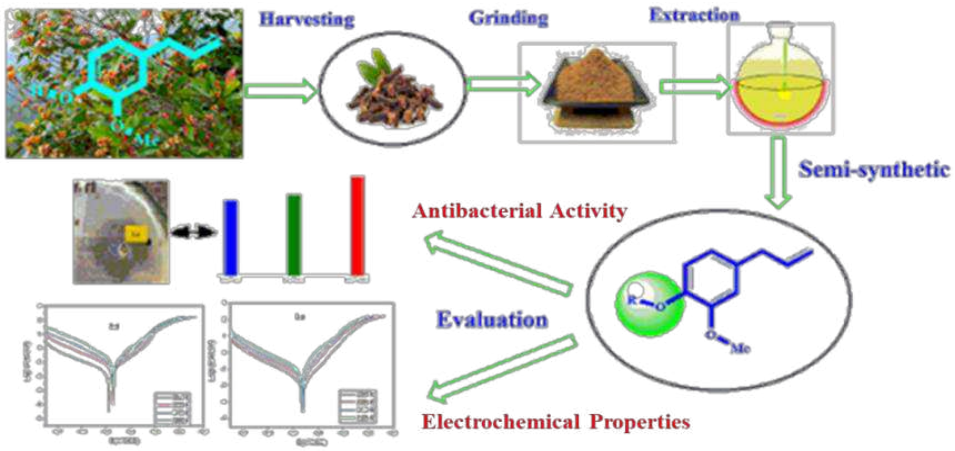

Figure 1. Design strategy, antibacterial activity, and anticorrosive efficacy of eugenol derivatives.

2. Results and Discussion

2.1. Chemistry

The new eugenol derivatives were synthesized using the synthetic route described in Scheme 1.

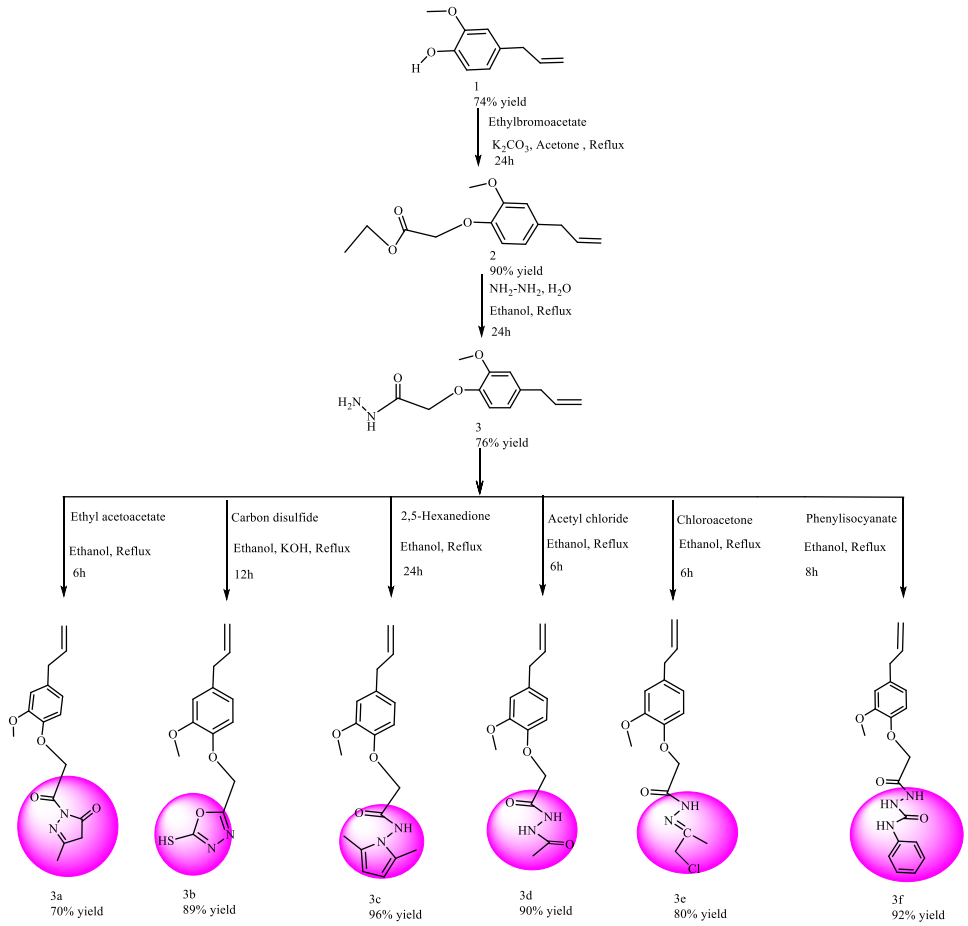

Schema 1. Synthetic route for the synthesis of eugenol derivatives.

Firstly, eugenol **1** was extracted from cloves by the hydrodistillation method with a 78% yield. The extracted product was used as the starting material for the synthesis of compounds **3a** to **3f**. Intermediates **2** and **3** were prepared and confirmed by comparing their melting points with the literature [3]. Compound **1** was reacted with ethyl bromoacetate in the presence of potassium carbonate and anhydrous acetone to give compound **2**, which was then treated with hydrazine monohydrate in ethanol to form compound **3**, the key intermediate, in 76% yield. This compound was used to give the final compounds **3a** to **3f**. Treatment of **3** with various reagents such as ethyl acetoacetate, carbon sulfide, hexane-2,5-dione, phenyl isocyanate, acetyl chloride, and chloroacetone in ethanol under reflux afforded compounds **3a** to **3f** in 70-96% yields and their structure was confirmed by analytical techniques such as FTIR, ^{1}H NMR, ^{13}C NMR. Some of these new compounds form crystals and their structure has been identified by X-ray diffraction [3] Haut du formulaire. The FTIR spectra showed significant signals for all the compounds synthesized. For example, compound **3a** exhibited bands at 1695 and 1665 cm-^{1}, confirming the presence of the characteristic C=O functions. Indeed, the ^{1}H NMR of product **3a** revealed peaks characteristic of methyl pyrazolone: a singlet at 3.6 ppm for the methyl group bound to pyrazolone, and a singlet at 3.25 ppm for the CH_2 ethyl group of pyrazolone. The ^{13}C NMR of compound **3a** reveals several characteristic peaks. In the strong fields, two peaks appear at 14.8 and 52 ppm; the peak at 14.8 ppm corresponds to the primary methyl carbon (CH_3) bound to the pyrazole ring, while the peak at 52 ppm corresponds to the secondary carbon (CH_2) characteristic of the pyrazole ring structure. In addition, low-field resonances at 168 and 165 ppm were attributed to the quaternary carbons (C=N) and (C=O) of the pyrazole ring, confirming cyclization and the formation of the pyrazole ring. When the ^{1}H NMR spectrum of compound **3b** was analyzed, various characteristic signals were identified, including an unshielded singlet at 14.5 ppm corresponding to the proton of the SH function. In the ^{13}C NMR spectrum of compound **3b**, significant signals were identified, including unshielded peaks corresponding to the quaternary carbons (C-O) and (C), at 178.2 and 160.3 ppm respectively. For compounds **3d**, **3e**, **3f**, ^{1}H and ^{13}C NMR analysis showed characteristic peaks for each compound. For example, for compound **3d**, a signal at 9.9 ppm appears for two protons of the secondary amines NH, as well as a singlet at 1.8 ppm for three protons of the

methyl group (CH_3). In addition, a shielded primary carbon peak is present at 20.9 ppm, and unshielded peaks of the quaternary carbons (C=O) and (C=O) appear at 167.2 and 168.5 ppm, respectively.

2.1. Microbiological Activity

In human and veterinary medicine, the resistance of infectious microorganisms to therapeutics has become a serious and growing health threat worldwide [20]. According to a WHO report, numerous actions have been launched to remedy this problem, despite all these efforts, there are still gaps in the excessive use of antibiotics and the limitation of the emergence of resistance to them (OMS, 2015). Our work consists of assessing the potential antibacterial properties of the synthesized compounds against several dangerous pathogenic bacteria such as S. aureus, E. coli, K. pneumonia, P. aeruginosa, and P. mirabilis. The findings required, from tested eugenol products and its derivatives, showed significant effectiveness against different studied pathogenic bacteria especially for concentrations of 100µg/mL (Table 1). In general, compounds 2, and 3, revealed an important antimicrobial activity against all negative and positive gram bacteria used in this study, with inhibition zones ranging from 13 mm (against E. coli) to 34 mm (against S. aureus). Here, the antimicrobial activities showed by compound 3 stay more courageous and advantageous than those revealed by compound 2 (Table 1).

Concerning compounds 3b and 3c, the final products of compound 3, were also effective against all tested pathogenic bacteria tested. However, compounds 3a and 3d, final products of compound 3, were only effective against negative-gram bacteria especially K. pneumonia (19 mm) and P. aeruginosa (22 mm) for compound 3a and E. coli (14 mm) and P. mirabilis (16mm) for compound 3d (Table 1). The derivative compound 3f was inactive against all tested pathogenic bacteria tested in this

study; while the derivative compound 3e showed only a moderate antimicrobial activity against S. aureus (positive-gram bacteria) (Table 1).

To improve activity against bacteria, incorporating the oxadiazole and pyrazole units is suggested to be achieved from a starting material such as hydrazide, which is considered highly effective. Conversely, some compounds showed poor activity in our trials. This could be related to low solubility or slow diffusion of the compounds in the agar.

In general, the absence or the reduced activity was mostly associated with compounds containing electron-withdrawing groups (NH, NH_2, NH-C(S)-NH, C=O, and C=S) or an electron-donating group. The presence of an electron-donating group (-Cl, $-CH_3$) in the synthesized compounds is considered very important, as it contributes to increasing their antimicrobial potential. Finally, the best inhibition properties against S. aureus, E. coli, and K. pneumoniae were observed for the heterocyclic compounds synthesized. According to Lagnika [17], a product is considered active if it has an inhibition diameter of more than 6 mm. In vitro, most of our compounds showed an important effectiveness against all dangerous pathogenic bacteria used in this study. Therefore, compounds 2, 3 and their derivatives, 3a, 3b, 3c, 3d, and 3e, could be considered as new active molecules against S. aureus, E. coli, K. pneumonia, P. aeruginosa, and P. mirabilis. Finally, these findings could be courageous and advantageous to use in vivo, as some alternative molecules, to treat infections caused by multidrug-resistant bacteria in the future.

Table 1. Zones of inhibition in (mm) for compounds 2, 3, 3a, 3b, 3c, 3d and 3f.

Zones of inhibition in (mm)					
Compounds	**S. aureus**	**E. coli**	**K. pneumoniae**	**P. mirabilis**	**P. aeruginosa**
DMSO	0	0	0	0	0
2	13±0.1 d	13±0.1 cd	19±0.1 cd	16±0.2 cd	15±0.4 cd
3	33±0.2 f	34±0.2 e	20±0.0 cd	25±0.0 cd	18±0.0 cd
3a	0 a	9±0.1 b	19±0.1 cd	10±0.3 cd	22±0.1 cd
3b	12±0.3 cd	13±0.1 cd	16±0.3 bc	18±0.3 bc	12±0.3 bc
3c	12±0.1 cd	12±0.1 bc	19±0.1 cd	14±0.3 cd	10±0.1 cd
3d	0 a	14±0.1 cd	12±0.0 b	16±0.1 b	10±0.0 b
3e	11±0.1 cd	0 a	0 a	0 a	0 a
3f	0	0	0	0	0

2.2. Electrochemical

2.2.1. Potentiodynamic Polarization Curves

This section of the research aims to comprehend the dynamics of metal corrosion and to explain the influence of the substituted heterocyclic compounds as inhibitors on the corrosion kinetics of carbon steel dissolution. Figures

2 show the polarization curves of the CS electrode in 1.0 mol/L HCl solution at 293 K without and with 10^{-3} M of each substituted heterocyclic compound, as the optimal concentration that corresponds to the maximum inhibition efficiency η%.

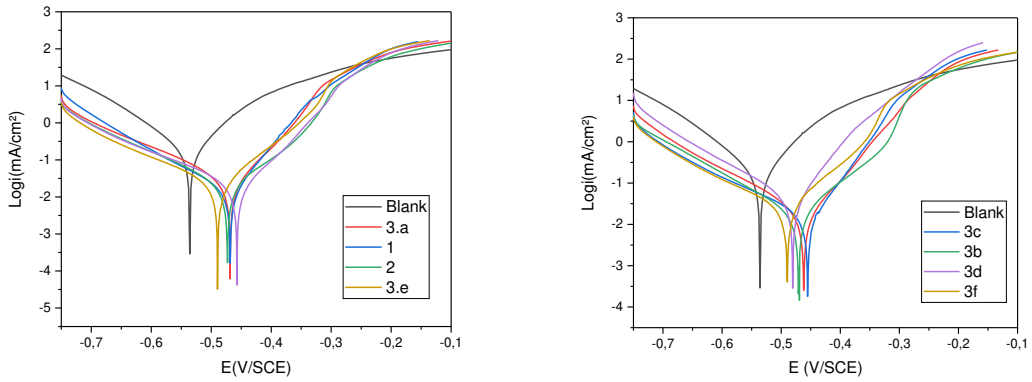

(a) (b)

Figure 2. Potentiodynamic polarization curves for carbon steel in 1.0 M HCl in the absence and presence of various compounds 3a, 2, 3, 3e, 3c, 3b, 3d, and 3f.

The corrosion parameters such as corrosion potential (Ecorr), corrosion current density (icorr), anode Tafel slope (ba), and cathode Tafel slope (bc), as well as the inhibition efficiency (η%), are listed in Table 2. The (η%) of the polarization curve test can be calculated using the formula below [21]:

$$(\eta\%) = \frac{Icorr - I'corr}{Icorr} * \mathbf{100} \qquad (1)$$

Where Icorr and I'corr are the corrosion current densities in the absence and presence of the inhibitors respectively.

Table 2. Electrochemical parameters for carbon steel in 1.0 M HCl at 293K.

Compounds	Icorr (µA/cm²)	-Ecorr (mV vs SCE)	ba (mV/dec)	-bc (mV/dec)	η%
Blanc	322.8	536.0	99.4	117.7	-
3a	34.5	468.4	62.7	160.9	89.31
3b	17.25	470.7	91.1	129.2	94.65
3d	15.61	489.3	78.5	122.9	95.16
3e	21.3	461.8	65.8	135.5	93.4
3c	39.3	480.5	61.0	121.3	87.82
2	12.8	468.6	53.2	110.2	96.03
3	13.36	472.9	82.4	97.1	95.8
3f	20.7	489.8	80.7	139.9	93.58

The polarization curves and electrochemical data reveal that when substituted heterocyclic compounds are added to the acid medium, the densities of the anodic and cathodic currents decrease significantly. This demonstrates that the existence of these inhibitors affects the surface of CS, implying that it can prevent iron oxidation and H^+ reduction during cathodic and anodic processes [22]. Based on the literature, when the displacement of Ecorr of inhibited solutions in comparison with the blank solution is bigger than 85 mV, the inhibitor is anodic or cathodic, whereas Ecorr shifts less than 85 mV can be explained by the inhibitor's mixed character [23]. The corrosion potential values did not fluctuate significantly in this investigation, and the displacement was less than 85 mV, showing that the substituted heterocyclic compounds acted as mixed-type inhibitors. It is observed that the current density decreases with inhibitor concentration. It decreases from 322.8 µA.cm^{-2} for a blank solution to 12.8 µA.cm^{-2} in the presence of 10^{-3} M of **2**. This result revealed that these inhibitors adsorb on the carbon steel surface and cover its active sites, resulting in the creation of a protective layer that reduces the reactivity of its dissolution. In actuality, inhibitory performance occurs in the following order: **2 > 3> 3d >3c > 3b > 3f > 3e > 3a**. Organic

compounds' inhibitory efficiency is known to be influenced by their size and/or the active centers included within their structure [24]. As a result, the presence of —CH_3 may be responsible for **2** 's superior inhibitory efficacy over other compounds. As a result, the presence of -CH_3 can enhance electron densities around the chemisorption center, whereas the presence of —OH, and —NO_2 can decrease the electronic density of these compounds [25].

2.2.2. Electrochemical impedance spectroscopy (EIS)

The stationary electrochemical approach is still insufficient for characterizing complex processes with many reaction steps and varying kinetics. Electrochemical impedance spectroscopy (EIS) is a useful tool for examining the adsorption process, electrode kinetics, and surface characteristics [21]. The Nyquist diagrams of carbon steel in 1.0 M HCl without and with the presence of 10^{-3} M of each substituted heterocyclic compound at 293K are represented in Figure 3.

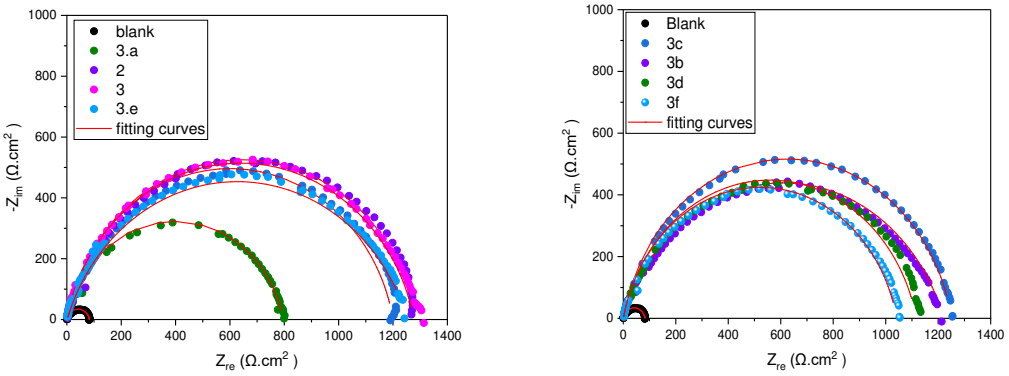

(a) *(b)*

Figure 3. Nyquist diagrams for carbon steel in 1.0 M HCl with the different compounds a (3a, 2, 3, 3e) and b (3f, 3c, 3b, 3d).

The Nyquist diagrams in 1M HCl medium indicate a capacitive loop whose diameter has changed significantly with the addition of all the inhibitors, with the maximum inhibitory efficiency found at 10^{-3} M of compound **2**. The presence of capacitive loops indicates that charge transfer controls steel corrosion [23]. Due to frequency dispersion and CS inhomogeneities, Nyquist graphs are not perfect capacitive loops [21].

Table 3 lists the different electrochemical parameters: Rs is the solution resistance, Rct is the charge transfer resistance, and Cdl is the constant-phase element of the double layer, as well as the inhibitory efficiency rate (η %) of steel corrosion in 1M HCl at 293K. The inhibitory efficiency was calculated according to the following equation [21]:

$$(\eta\%) = \frac{R_{ct} - R_{cto}}{R_{ct}} * 100 \qquad (2)$$

Where Rct0 and Rct represent the charge transfer resistance values in the absence and presence of an inhibitor, respectively.

Table 3. Inhibition efficiency and electrochemical data values for carbon steel in 1.0 M HCl before and after the addition of different compounds.

Compounds	Rs (Ω.cm²)	Rct (Ω.cm²)	C_{dl} (μF.cm²)	n	Q_{dl} ($\mu\Omega^{-1}cm^{-2}$ S^n)	η%
Blanc	0.58	82.33	253.1	0.88	401.6	
3a	1.375	794.5	50	0.86	76.39	89.63
3b	0.952	1220	46.86	0.79	84.5	93.25
3e	1.00	1252	60	0.79	100	93.42
3f	0.811	1041	52.19	0.87	75.93	92.09
2	0.85	1380	50.23	0.87	71.63	94.03
3	0.295	1280	25.48	0.86	40.83	93.56
3d	0.55	1116	43.69	0.861	66.84	92.62
3c	1.20	1250	54.27	0.87	75.2	93.41

According to the electrochemical parameters, the addition of inhibitors increases the transfer resistance Rct while decreasing the value of the double-layer capacitance (Cdl). Indeed, in the presence of 10^{-3} M compound **2**, the transfer resistance of the blank solution increases from 82.33 Ω.cm² to 1380 Ω.cm². This result can be explained by the reduction in the number of active sites (reduction of the local dielectric) on the surface of carbon steel due

to the adsorption of heterocycle derivatives on the metal surface [21]. On the other hand, it can be seen that the inhibition performance at 10^{-3} M of each inhibitor follows the tendency: **2> 3> 3f> 3c> 3b> 3d> 3f> 3a**, confirming the results obtained by the polarization measurements.

It is seen that these ten products are good corrosion inhibitors for carbon steel in 1.0 M HCl, where their inhibition efficiencies increase with concentration to reach maximum values of 94%, at 10^{-3} M of **2**.

2.2.3. Effect of temperature on inhibitor performance

The temperature reaction to the corrosion kinetic mechanism can offer information about the electrochemical characteristics of CS in the measured conditions. Because several inhibitor applications are performed at different temperatures depending on the steel's field of application, it would be interesting to investigate the effect of temperature on inhibitor performance [22]. Potentiodynamic polarization was used to determine the influence of temperature on the inhibition efficiency of carbon steel in 1M HCl containing 10^{-3} M of each compound at temperatures ranging from 293K to 323K (Figure 4).

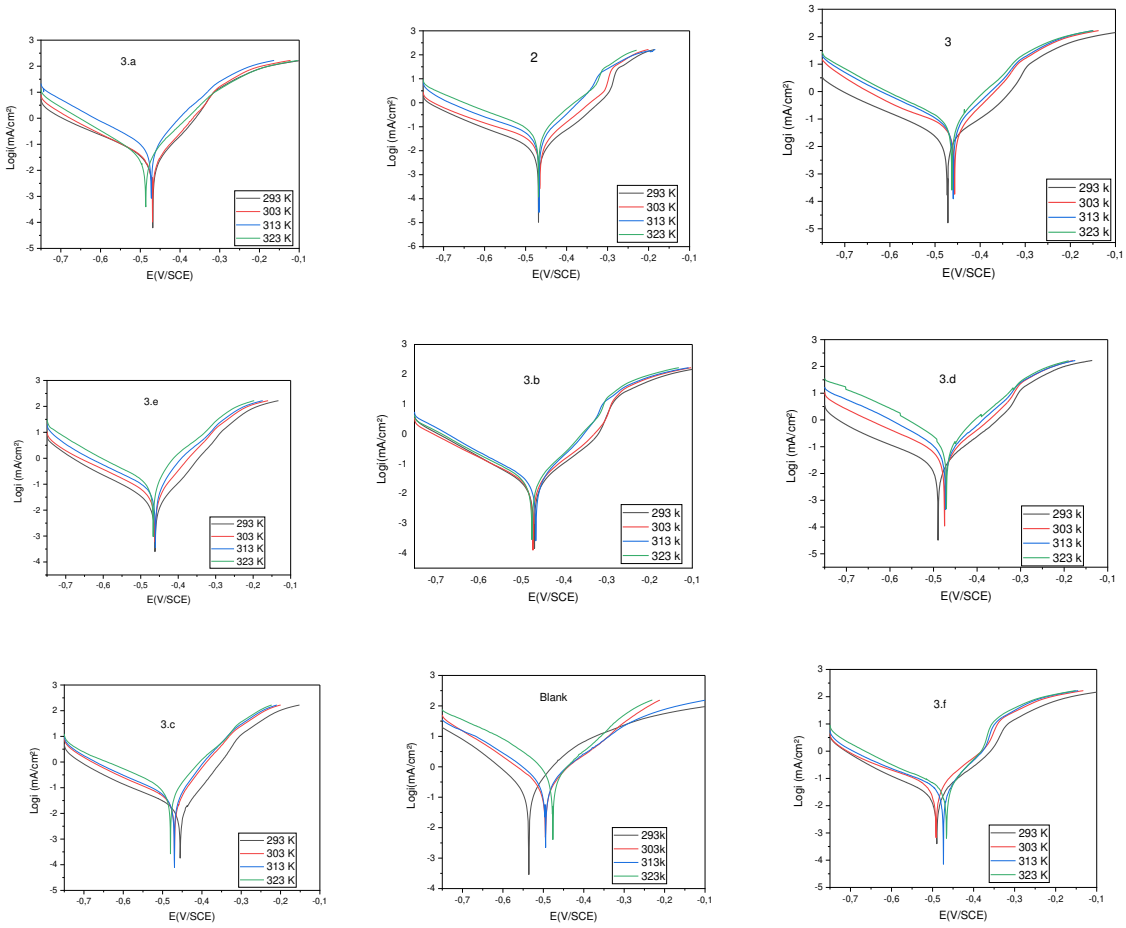

Figure 4. Electrochemical parameters of CS in the HCl 1M and HCl 1M + 10^{-3} M of each compound at different temperature ranges.

The electrochemical parameters of polarization curves are summarized in Table 4

Table 4. Electrochemical parameters of CS in the HCl 1M and HCl 1M +10^{-3} M of each compound at different temperature ranges.

Compounds	T (K)	Icorr(µA/cm²)	-Ecorr(mV vs SCE)	ba (mV/dec)	-bc (mV/dec)	η%
Blanc	293	322.8	536.0	99.4	117.7	-
	303	417.6	494.7	106.0	132.9	-
	313	557.7	494.4	121.3	145.3	-
	323	1419.0	476.5	113.7	160.4	-
3a	293	34.5	468.4	62.7	160.9	89.31
	303	30.5	469.0	63.8	136.1	92.69
	313	85.4	472.5	64.0	118.3	84.68
	323	120.6	486.3	69.3	110.8	91.50
3b	293	17.25	470.7	91.1	129.2	94.65
	303	21.52	472.9	89.6	143.3	94.84
	313	48.6	466.0	73.5	132.2	91.28
	323	89.5	475.0	72.3	111.2	93.69
3d	293	15.61	489.3	78.5	122.9	95.16
	303	36.22	475.0	71.1	94.5	91.32
	313	56.1	472.4	69.0	89.5	89.94
	323	123.4	470.1	70.7	94.9	91.3
3e	293	21.3	461.8	65.8	135.5	93.40
	303	44.2	461.8	65.4	148.8	89.41
	313	59.0	460.8	65.9	142.5	89.4
	323	86.8	466.7	67.1	129.4	93.88
2	293	12.8	468.6	53.2	110.2	96.03
	303	18.80	465.3	71.7	156.3	95.4
	313	36.6	467.4	56.3	165.5	93.43
	323	51.9	468.6	67.0	140.6	96.34
3	293	13.36	472.9	82.4	97.1	95.8
	303	45.7	456.7	66.0	155.1	89.05
	313	52.1	459.7	64.7	118.7	90.65
	323	62.8	462.7	59.1	107.7	95.57
3f	293	20.7	489.8	80.7	139.9	93.58
	303	57.6	491.5	91.5	198.5	86.20
	313	82.6	473.9	69.4	164.4	85.18
	323	77.5	466.0	59.0	142.0	94.53
3c	293	17.0	455.2	54.3	159.41	94.7
	303	34.4	469.7	55.6	150.4	91.76
	313	37.9	470.5	52.9	142.5	93.20
	323	92.4	480.0	72.6	154.6	93.48

For all the compounds, it is noticed that the catholic and anodic branches of the polarization curves present a Tafel region. This discovery indicates that the reduction and oxidation reactions occur according to a kinetic process of pure activation. The results indicate that higher temperatures did not cause a significant decrease in inhibitory inhibition in the presence of 10^{-3} M of substituted heterocyclic compounds. This shows that the inhibitory compounds acted on the carbon steel surface via adsorption in HCl. The results obtained showed that the inhibitors used provide sufficient protection against corrosion even at high temperatures.

2.2.4. Thermodynamic activation parameters

In order to examine the corrosion process and determine the thermodynamic parameters, we will study the effect of temperature on corrosion current density. The rate of corrosion obeys Arrhenius' law expressed by the corrosion current density given by the following relationship:

$$\text{icorr} = \text{A}.\, e^{\frac{(-\text{Ea})}{\text{R.T}}} \qquad (3)$$

Where icorr is the corrosion current density; Ea is the apparent activation energy; A is a constant; R is the universal perfect gas constant (8.314 J.mol^{-1}. K $^{-1}$); T is the temperature (K).

Semi-logarithmic representations of the corrosion current density as a function of the inverse of the blank temperature and in the presence of inhibitors are shown in Figures 4 and 5. These representations are straight lines with slope -Ea/R, enabling the apparent activation energy to be calculated.

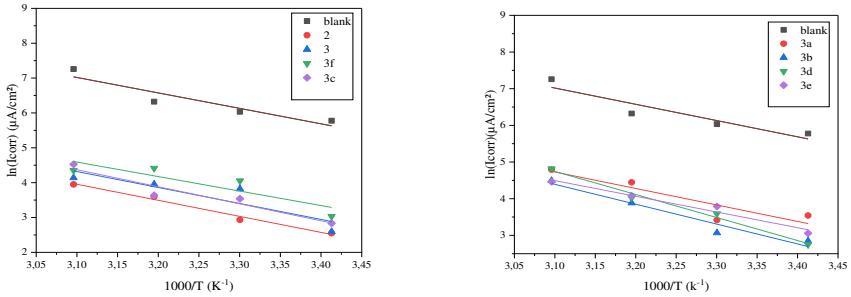

(a) *(b)*

Figure 5. Arrhenius plots generated from the corrosion current density of steel in a 1M HCl environment, with the presence of inhibitors (2,3, 3a, 3b, 3c, 3d, 3e, 3f).

Comparison of the activation energy values obtained without (Ea) and in the presence of inhibitor (Eai) enables the mechanism of inhibitor protection to be predicted as a function of temperature. In 1965, Radovici proposed a classification of inhibitors according to their Ea:

- Eai > Ea: the inhibitor adsorbs to the substrate via electrostatic-type bonds (weak bonds). This type of bond is sensitive to temperature (physisorption).
- Eai < Ea: the inhibitor's protective power increases with temperature. The inhibitor molecules adsorb to the metal surface via strong bonds (chemisorption).
- Eai = Ea: the inhibitor has a mixed character (physical and chemical adsorption). Very few compounds fall into the latter category.

The increase in apparent activation energy in the presence of an inhibitor compared to blank indicates poor inhibitor performance as T increases. This can be interpreted as an electrostatic adsorption process of the inhibitor to the steel surface (physisorption).

Other thermodynamic parameters can be determined from the Arrhenius equation, namely enthalpy and entropy values

$$icorr = \frac{RT}{Nh} exp\ (\frac{\Delta S*}{R})\ \exp\ (-\frac{\Delta H*}{RT}) \qquad (4)$$

Where h: Planck's constant ($6.62607004 \times 10^{-34}$ J.s), N is Avogadro's number (6.02 mol^{-1}), ΔS^* is the entropy of activation, $\Delta H*$ is the enthalpy of activation, T is the temperature; R is the perfect gas constant (8.31 $J.mol^{-1}.K^{-1}$). To determine the enthalpy and entropy, simply plot the curve Ln (Icorr/T)= f(1000/T) (see Figure 6).

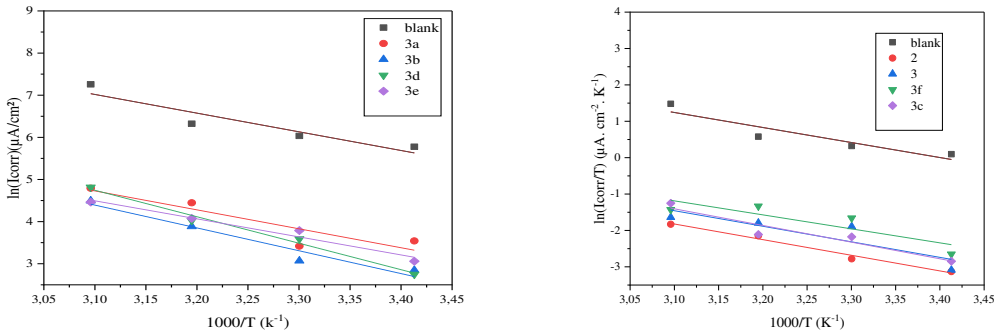

Figure 6. Arrhenius curves derived from the corrosion current density of steel in a 1M HCl solution, with the addition of inhibitors (2,3, 3a, 3b, 3c, 3d, 3e, 3f).

The values of the thermodynamic parameters Ea, ΔH^*, and ΔS^* in 1M HCl medium without and in the presence of the inhibitors are grouped in Table 5.

Table 5. Thermodynamic parameters of steel in 1 M HCl both in the absence and presence of inhibitors.

Compounds	Ea (kJ/mol)	ΔH*a (kJ/mol)	ΔS *a (J/mol.K)	Ea -ΔH*a
Blanc	36.86	34.3	-80.86	2.56
3a	37.37	34.81	-98.32	2.56
3b	45.03	42.48	-77.33	2.55
3d	52.24	49.68	-52.08	2.56
3f	38.58	36.02	-105.79	2.56
2	38.27	35.72	-101.95	2.55
3	38.08	35.52	-99.53	2.56
3e	38.99	36.43	-108.27	2.56
3c	40.61	38.43	-91.25	2.18

Le signe positif de ΔH*a reflète la nature endothermique du processus de dissolution de l'acier. Cependant, la valeur enthalpique en présence d'inhibiteurs est plus élevée que celle obtenue en l'absence d'inhibiteurs (36,86 kJ/mol), une évolution attribuée à l'adsorption physique des molécules d'inhibiteurs sur la surface de l'acier. Les valeurs négatives de ΔS*a montrent qu'il y a une augmentation du désordre lors de la formation de réactifs complexes actifs en solution.

2.2.5. Immersion time effect

The effect of immersion time on the inhibition efficiency of eugenol-based heterocyclic compounds (2, 3, 3a, 3b, 3c, 3d, 3e, 3f) was studied. The Nyquist diagrams of carbon steel in 1M HCl with and without the addition of heterocyclic compound inhibitors for different immersion times ranging from 30 min to 24 h are presented in Figure 7. The characteristic parameters of these curves are shown in Table 6.

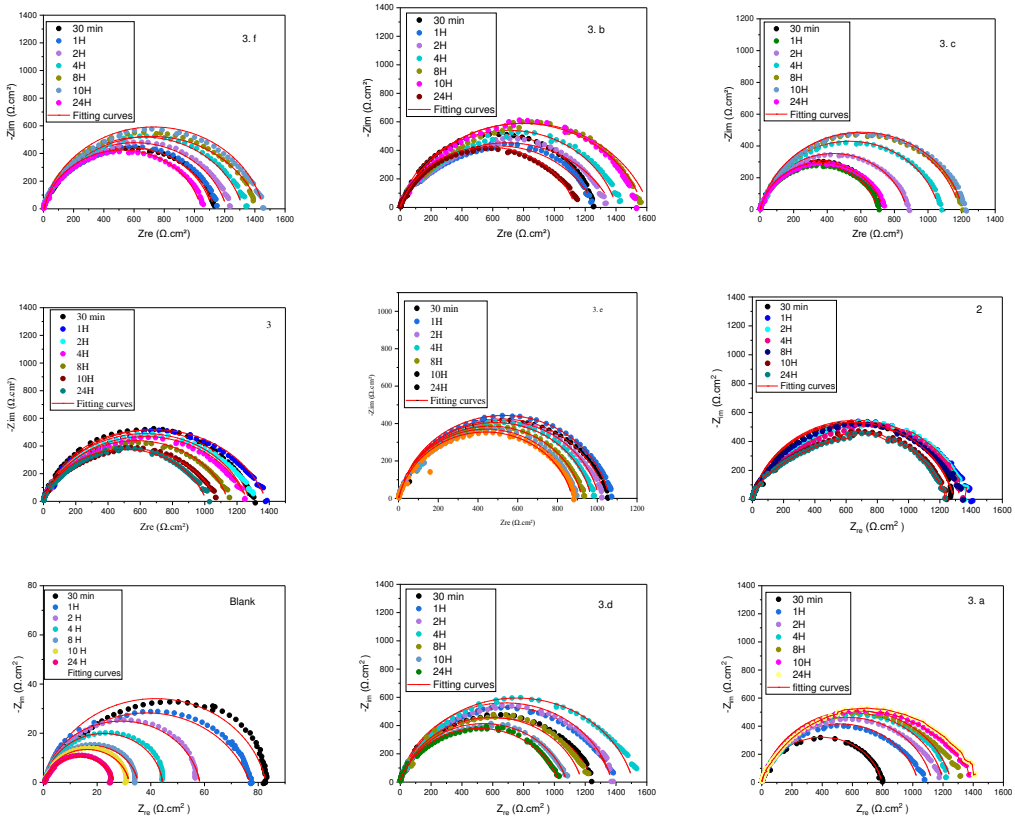

Figure7. Nyquist diagram obtained at different immersion times for eugenol derivatives.

Table 6. Electrochemical parameters of heterocyclic compounds and blank (1M HCl) as a function of immersion time.

Compounds	Immersion time	Rs(Ω.cm^2)	Rct(Ω.cm^2)	Cdl(µF.cm^{-2})	n	Qdl(µΩ^{-1}. cm^{-2}. Sn)	η%
Blank (HCl 1M)	30 min	0.58	82.33	253.1	0.88	401.6	/////
	1 H	0.20	77.86	118.6	0.84	247.6	/////
	2 H	0.95	57.99	261	0.92	363.4	////
	4 H	1.06	43.91	365.2	0.96	425.9	///
	8 H	0.69	38.64	472.5	0.91	669.6	////
	10 H	0.70	33.46	569.1	0.95	697.1	///
	24 H	0.54	25.36	1510	0.87	2301	////
3a	30 min	1.37	794.5	50	0.86	76.39	89.63
	1 H	0.65	1035	49.42	0.86	74.53	92,47
	2 H	0.15	1129	41.97	0.87	61.37	94.86
	4 H	0.63	1204	43.82	0.87	63.19	96.35
	8 H	0.14	1255	41.13	0.87	60.34	96.9
	10 H	0.45	1313	41.72	0.86	62.43	97.45
	24 H	0.43	1354	40.75	0.85	61.6	98 .12
2	30 min	0.85	1287	50.23	0.87	71.63	93.60
	1 H	1.10	1333	26.06	0.87	39.64	94.15
	2 H	0.64	1319	25.56	0.87	39.89	95.60
	4 H	0.32	1291	25.66	0.87	40.53	96.59
	8 H	0.109	1291	29.66	0.87	44.02	97.00
	10 H	0.23	1189	25.9	0.86	41.85	97.18
	24 H	0.43	1171	26.86	0.86	44.1	97.83
3	30 min	0.29	1280	25.48	0.86	40.83	93.56
	1 H	0.98	1392	26.49	0.87	48.71	94.40
	2 H	0.34	1266	30.51	0.87	51.63	95.41
	4 H	1.14	1263	34.51	0.81	62.15	96.52
	8 H	0.24	1146	38.85	0.83	65.37	96.62
	10 H	0.21	1076	66.11	0.85	62.14	96.89
	24 H	0.57	1017	37.44	0.86	69.5	97.50
3d	30 min	1.00	1252	60	0.79	100	93.42
	1 H	2.05	1355	37.83	0.81	65.5	95.25
	2 H	1.65	1379	28.47	0.87	43.42	95.79
	4 H	0.74	1512	28.4	0.85	45.6	97.09
	8 H	1.6	1179	32.62	0.84	54.55	96.72
	10 H	1.57	1081	24.6	0.85	44.18	96.90
	24 H	1.5	1035	22.48	0.86	46.51	97.54
3e	30 min	0.81	1041	52.19	0.87	75.93	92.09
	1 H	0.84	1060	46.53	0.89	65.34	92.65
	2 H	0.85	1009	50.12	0.88	71.86	94.25
	4 H	0.52	969.6	65.9	0.88	74.45	95.47
	8 H	0.51	922.8	68.8	0.88	76.85	95.8
	10 H	0.46	882.6	75.2	0.88	82.45	96.20
	24 H	0.76	874.8	75.9	0.86	83.78	97.10
3c	30 min	1.20	1250	54.27	0.87	75.2	93.41
	1 H	2.26	1261	57.22	0.810	77.3	93.82
	2 H	1.94	1377	43.79	0.81	73.54	95.78
	4 H	1.5	1399	37.94	0.83	61.1	96.86
	8 H	2.03	1614	32.14	0.80	55.48	97.60
	10 H	1.8	1569	45.15	0.82	66.12	97.86
	24 H	1.11	1098	42.13	0.85	66.87	97.69
3b	30 min	1.156	710	55.64	0.91	73.06	88.40
	1 H	0.71	698.2	75.51	0.86	89.58	88.84
	2 H	0.88	873.8	73.93	0.86	88.45	93.36
	4 H	1.07	1066	60.59	0.86	87.78	95.88
	8 H	1.19	1188	54.35	0.86	78.74	96.74
	10 H	1.21	1206	53.57	0.86	77.6	97.22
	24 H	0.74	734	88.01	0.86	99.64	96.51

The results revealed that immersion time had a considerable impact on the size of the impedance spectrum, as illustrated in Figure 7. The capacitive loops were the same shape in both uninhibited and inhibited solutions, indicating that carbon steel corrosion was mainly controlled by the charge transfer process over time.

The results obtained from this study showed that the compounds have a stable long-term inhibition effect. According to Chafiq et al., this is mainly due to a large number of unoccupied or vacant sites[26].

3. Experimental

3.1. Experimental details of chemicals

Melting points were measured using a capillary tube on the Buchi-Tottoli apparatus. IR spectra were measured using a Fourier transform infrared spectrophotometer (JASCO FT/IR 4600 Type A) fitted with an ATR accessory. FTIR spectra were recorded in the 4000-500 cm^{-1} region with a resolution of 4 cm^{-1}. ^{1}H and ^{13}C NMR spectra were recorded in DMSO-d_6 using a Bruker AC 500 MHz instrument for ^{1}H and 120 MHz for ^{13}C. Chemical shifts are given in ppm relative to tetramethylsilane (TMS) taken as the internal reference.

3.1.1. Preparation of ethyl 2-(4-allyl-2-methoxyphenoxy) acetate (2)

Anhydrous potassium carbonate (5.21g, 0.045mol) and eugenol (5g, 0.03mol) were mixed in acetone (150 mL) in a (200 mL) flask with stirring at room temperature. After 15 min ethyl bromoacetate (5.01 g, 0.03 mol) was added to the mixture and the solution refluxed for 24 hours. The mixture was cooled to room temperature and the solvent was removed under reduced pressure. The residual mass was triturated with ice-cold water to remove potassium carbonate and extracted with ether (3 × 50 mL), then dried over anhydrous sodium sulfate and evaporated to dryness to give a brown oil. The synthesized product was purified by silica gel column chromatography using a hexane/ethyl acetate (8/2) solvent mixture as the eluent and recrystallized in ethanol. The brown oily product obtained in 90% yield. $C_{14}H_{18}O_4$. MW=250.12g/mol. IR (n, cm^{-1}, KBr) : 1731(C=O). ^{1}H NMR (500 MHz, DMSO-d_6, ppm) : δ 6.82 (^{1}H, d, C-H, J= 4.4 Hz), 6.80 (^{1}H, d, C-H, J= 4.4 Hz), 6.70 (^{1}H, s, C-H), 5.90 (^{1}H, m, C-H), 5.01-4. 95 (^{2}H, m, CH_2), 4.6 (2H, s, C-H), 4.26 (2H, q, C-H, J= 7.8 Hz), 3.7 (3H, s, CH_3), 3.29 (2H, d, J= 6.73Hz, CH_2), 1.16 (3H, t, CH_3, J= 7.8Hz). ^{13}C NMR (125 MHz, DMSO-d_6, ppm) : δ 169.17 (C=O), 149.9 (C), 146.2 (C), 138.8 (CH), 134.5 (C), 122. 5 (CH), 115.5 (CH_2), 115.2 (CH), 113.8 (CH), 65.7 (O-CH_2), 61.11(CH_2), 56.1 (O-CH_3), 39.8 (CH_2), 14.1 (CH_3).

3.1.2. Preparation of 2-(4-allyl-2-methoxyphenoxy) acetohydrazide (3)

The compound ethyl 2-(4-allyl-2-methoxyphenoxy) acetate (4.5 g, 0.017 mol) was combined with 98% hydrazine monohydrate (2 mL, 0.04 mol) and absolute ethanol (30 mL) in a 100 mL flask and heated under reflux for 24 hours. The reaction mixture was cooled, and the solid formed was filtered, dried, and recrystallized from acetic acid, giving compound **3**. Purification of the synthesized product was carried out by silica gel column chromatography, using a mixture of solvents (chloroform/dichloromethane) as the eluent. The product obtained was a white solid with a 76% yield. $C_{12}H_{16}N_2O_3$. MW = 236.12 g/mol. m p: 142-143 °C. IR (n, cm^{-1}, KBr) : 3411.18 (-$NHNH_2$), 1680.66 (C=O). ^{1}H NMR (500 MHz, DMSO-d_6, ppm) : δ 9.01 (1H, s, NH), 6.82 (1H, d, CH, J= 4.4 Hz), 6.80 (1H, d, CH, J= 4.4 Hz), 6.70 (1H, s, CH), 5.80 (1H, m, CH), 5. 01-5.02 (2H, m, CH), 4.9ppm (2H, s, NH_2), 4.39 (2H, s, CH_2), 3.7 (3H, s, CH_3), 3.2 (2H, d, J = 6.8 Hz, CH_2). ^{13}C NMR (125 MHz, DMSO-d_6, ppm) : δ 167.9(C=O), 150(C), 146.2 (C), 138 (CH), 134 (C), 121.9(CH), 115.9 (CH_2), 115 CH), 113 (CH), 68 (CH_2), 56.01 (O-CH_3), 40.01 (CH_2).

3.1.3. Preparation of 2-(2-(4-allyl-2-methoxyphenoxy) acetyl)-5-methyl-1,2-dihydro-3H-pyrazole-3-one (3.a)

The compound 2-(4-allyl-2-methoxyphenoxy) acetohydrazide (0.7 g, 0.003 mol) was heated with ethanol (50 mL) and ethyl acetoacetate (0.40 g, 0.003 mol) in a 100 mL flask at reflux for 6 hours. The cooled solution was subjected to evaporation of the solvent by rotary steaming. The synthesized product was purified by silica gel column chromatography using a hexane/ethyl acetate (9/1) solvent mixture and recrystallized in ethanol. The product obtained is a yellow solid with a 70% yield. $C_{16}H_{18}N_2O_4$. MW = 302.13 g/mol. m p: 275-276 °C. IR (n, cm^{-1}, KBr): 1695 et 1665 (C=O). ^{1}H NMR (500 MHz, DMSO-d_6, ppm) : δ 6.83(1H, d, CH, J =4.6 Hz), 6.81(1H, d, CH, J = 4.6 Hz), 6.74 (1H, s, CH), 5.90 (1H, m, CH), 5.0-5.01 (2H, m, CH_2), 4.6 (2H, s, CH_2), 3.7 (3H, s, CH_3), 3. 6 (3H, s, CH_3), 3.26 (2H, d, CH_2, J = 8.6 Hz). ^{13}C NMR (125 MHz, DMSO-d_6, ppm) : δ 170(C=O), 168(C), 165(C=O), 150(C), 145.9(C), 139(CH), 134(C), 121.9(CH), 116(CH_2), 115(CH), 113(CH), 66(CH_2), 56(O-CH_3), 52(CH_2), 39(CH_2), 14.8(CH_3).

3.1.4. Preparation of 5-((4-allyl-2-methoxyphenoxy) methyl)-1,3,4-oxadiazole-2-thiol (3.b)

A solution of 2-(4-allyl-2-methoxyphenoxy) acetohydrazide (2.1 g, 0.008 mol) in 50 ml ethanol, in the presence of potassium hydroxide (0.45 g, 0.008 mol) and excess carbon disulfide (0.61g, 0.08 mol), was heated under reflux for 12 hours. After the concentrated solution had cooled, it was poured over ice-cold water (50 mL), and acidified with 2 mL acetic acid. Liquid-liquid extraction with dichloromethane (3 times 50 mL) was followed by evaporation of the solvent by rota steam, resulting in a powder product. The synthesized product was purified by chromatography on silica gel, using a mixture of hexane/ethyl acetate solvents (9/1) recrystallized in ethanol. The product obtained as a yellow powder in RT yield: 89%. $C_{13}H_{14}N_2O_3S$. MW=278.07g/mol. m p: 208-209°C. IR (n, cm^{-1}, KBr) : 3460 (NH), 1656.7 (C=N), 1580 (C=C), 1560.3 (C=N). ^{1}H NMR (500 MHz, DMSO-d_6, ppm) : δ 14.5 (1H, s, SH), 6.90 (1H, d, CH, J = 4.5 Hz), 6.88 (1H, d, CH, J =4.5 Hz), 6.76 (1H, s, CH), 5.90 (1H, m, CH), 5.01-5.08 (2H, m, CH_2), 5.08 (2H, s, CH_2), 3.7 (3H, s, CH_3), 3.2 (2H, d, CH_2, J =6.8 Hz). ^{13}C NMR (125 MHz, DMSO-d_6, ppm): δ 178.2(C-S), 160.3 (C), 150.2 (C), 145.02 (C), 138.1 (C), 135.9 (CH), 121.5 (CH), 116.2 (CH), 115.9 (CH_2), 113.1 (CH), 61.9 (CH_2), 56.03 (CH_3), 39.8 (CH_2).

3.1.5. Preparation of 2-(4-allyl-2-methoxyphenoxy) - N-(2,5-dimethyl-1H-pyrrole-1-yl)acetamide (3.c)

A solution of 2-(4-allyl-2-methoxyphenoxy) acetohydrazide (0.6g, 0.0025mol) and hexane-2,5-dione (0.43g, 0.0037mol) in a 100 mL flask containing ethanol was heated under reflux for 24 hours. The cooled solution was

concentrated by rotary evaporation of the solvent. The synthesized product was purified by silica gel column chromatography, using a hexane/ethyl acetate (9/1) solvent mixture, and crystallized in ethyl acetate. The product was obtained as a White Crystal with a 96% yield. $C_{18}H_{22}N_2O_3$. MW=314.16g/mol. m p: 251-252°C. IR (n, cm^{-1}, KBr) : 3460 (NH), 1710 (C=O), 3157 (C=CH), 2960 (CH_3), 1616 (C=C), 1503 (C=C). ^{1}H NMR (500 MHz, DMSO-d_6, ppm) : δ10.8 (1H, s, NH), 6.88 (1H, d, CH, J =4.5 Hz), 6.86 (1H, d, CH, J =4.5 Hz), 6.78 (1H, s, CH), 5.90 (1H, m, CH), 5.59 (2H, s, CH, CH), 5. 01-5.02 (2H, m, CH), 4.67 (2H, s, CH_2), 3.68 (3H, s, CH_3), 3.30 (2H, d, CH_2, J = 6.7Hz), 1.91 (6H, s, CH_3, CH_3). ^{13}C NMR (125 MHz, DMSO-d_6, ppm): δ169.8 (C), 150.1 (CH), 147.1 (C), 139.1 (CH), 135.8 (C), 127.9 (C, C), 121.5 (CH), 116.2 (CH_2), 116 (CH), 113 (CH), 104.7 (CH, CH), 68.1 (CH_2), 10.2 (CH_3, CH_3).

3.1.6. Preparation du N'-acetyl-2-(4-allyl-2-methoxyphenoxy)acetohydrazide (3.d)

A solution of 2-(4-allyl-2-methoxyphenoxy) acetohydrazide (0.67g, 0.003 mol) in 50ml ethanol, in the presence of acetyl chloride (0.22 g, 0.003 mol) in a 100 mL flask, was heated under reflux for 6 hours. The cooled solution was then concentrated by rotary evaporation of the solvent. The synthesized product was purified by chromatography on a silica gel column, using a mixture of hexane/ethyl acetate solvents (9/1). The product was obtained as a white solid with a 90% yield. $C_{14}H_{18}N_2O_4$. PM 278,13 g/mol. m p: 256-257°C. IR (n, cm^{-1}, KBr) : 3314 (NH), 1528 (C=O), 1183 (N-N) ,1082 (N-C). ^{1}H NMR (500 MHz, DMSO-d6, ppm): δ 9.9 (2H, s, NH-NH), 6.84 (1H, d, CH, J = 4.5 Hz), 6.82 (1H, d, CH, J = 4.5 Hz), 6.76 ppm (1H, s, CH), 5.89 (1H, m, CH), 5.01-5.03 (2H, m, CH_2), 4.6 (2H, s, CH_2), 3.7 (3H, s, CH_3), 3.25 (2H, d, CH2, J =6.8 Hz), 1.8 (3H, s, CH_3).^{13}C NMR (125 MHz, DMSO-d_6, ppm) : δ 168.5 (C=O) ; 167.2 (C=O) ; 149.1 (C) ; 146.4 (C) ; 138.3 (CH2) ; 134.2 (C) ; 120.6 (CH), 116.1 (CH2) ; 114.6 (CH) ; 112.6 (CH) ; 67.8 (CH_2) ; 56.9 (O-CH_3) ; 39.6 (CH_2) ; 20.9 (CH_3).

3.1.7. Preparation of (Z)-2-(4-allyl-2-methoxyphenoxy)-N'-(1-chloropropan-2-ylidene) acetohydrazide (3.e)

A solution of 2-(4-allyl-2-methoxyphenoxy) acetohydrazide (3.06 g, 0.012 mol) in 50ml ethanol, combined with chloroacetone (1.11 g, 0.012 mol) in a 100 mL flask, was heated under reflux for 6 hours. After cooling, the solvent was concentrated by vacuum evaporation using a steam rota. The synthesized product was purified by silica gel column chromatography using a hexane/ethyl acetate (9/1) solvent mixture and recrystallized in methanol. The product was obtained in the oily yellow form with an 80% yield. $C_{13}H_{15}ClN_2O_3$. MW=282.08g/mol. IR (n, cm^{-1}, KBr): 1760 (C=N), 1688 (C=O), 840 (Cl-C). ^{1}H NMR (500 MHz, DMSO-d_6, ppm): δ 9.95 (1H, s, NH) ; 6.86 (1H, d, CH, J = 4.5Hz), 6.88 (1H, d, CH, J = 4.5 Hz), 6.78 (1H, s, CH), 5.90 (1H, m, CH), 5.02-5.04 (2H, m, CH_2), 4.6 (2H, s, CH_2), 4.2 (2H, s, CH_2), 3.74 (3H, s, CH_3), 3.25 (2H, d, CH_2, J =6.8 Hz), 1.1 (3H, s, CH_3). ^{13}C NMR (125 MHz, DMSO-d_6, ppm) : δ 169.3 (C=O), 163.3 (C), 149.2 (C), 146.4 (C), 136.4 (CH), 133.9 (C), 120.4 (CH), 116.07 (CH_2), 114.9 (CH), 113.9 (CH), 66.07 (CH_3), 61.01 (CH_2), 56.01 (CH_3), 39.7 (CH_2), 14.5 (CH_2).

3.1.8. Preparation of 2-(2-(4-allyl-2-methoxyphenoxy)acetyl)-N-phenyl hydrazine-1-carboxamide (3.f)

A solution of 2-(4-allyl-2-methoxyphenoxy) acetohydrazide (0.67 g, 0.003 mol) in 50ml ethanol, in the presence of phenyl isocyanate (0.33 g, 0.003 mol) in a 100 mL flask, was heated under reflux for 8 hours. The cooled solution was concentrated by rotary evaporation of the solvent. Purification of the synthesized product was carried out by silica gel column chromatography, using a hexane/ethyl acetate (9/1) solvent mixture. The product was obtained as a White Solid with a 92% yield. $C_{19}H_{21}N_3O_4$ .PM=355.15 g/mol. m p: 280-281°C. IR (n, cm^{-1}, KBr) :3179, 3299 and 3316 (NH), 1644 (C=O), 1547 (C-N). ^{1}H NMR (500 MHz, DMSO-d_6, ppm) : δ 11.2 (1H, s, NH), 10.5 (1H, s, NH), 9.75 (1H, s, NH), 7.50 (2H, d, CH, CH, J=10 Hz), 7.37 (2H, dd, CH, CH, J=10 Hz), 7.07 (1H, dd, CH, J=10 Hz), 6.88 (1H, d, CH, J =4.5 Hz), 6.85 (1H, d, CH, J = 4.5 Hz), 6.76 (1H, s, CH), 5.90 (1H, m, CH), 5.06-5.04 (2H, m, CH_2), 4.5 (2H, s, CH_2), 3.73 (3H, s, O-CH_3), 3.29 (2H, d, CH_2, J = 6.8Hz). ^{13}C NMR (125 MHz, DMSO-d_6, ppm) : *δ168*.32 (C=O), 162.8 (C=O), 150.4 (C), 145.87 (C), 139.4 (C), 138.46 (CH), 133.9 (C), 128 (CH), 128 (CH), 127.1 (CH), 121.6 (CH), 121.6 (CH), 121.58 (CH), 115.6(CH_2), 113.3 (CH), 114.8 (CH), 68.11 (CH_2), 56.09 (CCH_3), 39 (CH_2).

3.2. Experimental details of microbiological activity

The antibacterial activity of the synthesized compounds was tested against three pathogenic bacterial strains: Staphylococcus aureus (ATCC-29213), Escherichia coli (ATCC-25922), and Klebsiella pneumoniae (ATCC-700603). The in vitro antimicrobial activity of eugenol derivatives was estimated using the well diffusion method [27]. After solidification of the nutrient agar plates, 1 ml of each bacterial solution was poured and spread in the Petri dish. Next, we drilled wells (8 mm diameter) in the agar plates using a sterile cork borer to pour 100 µL of each test compound into each well. Petri plates were incubated at 36ºC for 24 h. After incubation, the diameter of growth inhibition zones was measured after 24 h for all pathogenic microorganisms. For each sample and bacterial species, three duplicates were kept.

3.3. Electrochemical Measurements

3.3.1. Materials and Electrolyte Preparation

In the present investigation, carbon steel (CS) specimens with the following composition (weight%): 0.07 C, 0.19 Mn, 0.03 Si, 0.05 Cr, 0.02 Al, and balance Fe were utilized. Before starting each electrochemical test, the CS electrode was meticulously polished with emery papers ranging in roughness from N° 180 to N° 2500. Then the polished electrode was washed with distilled water, degreased with acetone, and dried with heated air. The aggressive 1 M HCl solution was prepared by diluting HCl grade 37% (purchased from LOBA Chemie Company) with distilled water. Each test was carried out with a freshly obtained solution.

3.3.2. Electrochemical Measurements

Electrochemical methods were utilized to assess the immediate rate of corrosion and explain the effect of the inhibitors on the CS corrosion process. All electrochemical experiments were conducted using Potentiostat type OrigaStat 100, controlled by Origamaster5 software. The cell used three electrodes consisting of a working electrode (carbon steel), a platinum electrode as a counter electrode, and a saturated calomel electrode (SCE) as a reference electrode. The working electrode surface area exposed to the electrolyte was 0.64 cm^2. Open circuit potential (OCP) surveillance was performed by immersing the working electrode in the corrosive medium in the absence and existence of inhibitors for 30 min. The potentiodynamic polarization (PDP) curves of the CS electrode in 1.0 M HCl, without and with inhibitors, were recorded in the potential range from -750 to -100 mV/SCE, at the scan rate of 1 mV/s. Electrochemical impedance spectroscopy investigations were carried out by applying a signal amplitude perturbation of 10 mV, in the frequency range of 1kHz to 100 mHz. The temperature effect on the inhibitor performance was evaluated in the range from 293 to 323 K.

4. Conclusion

In conclusion, six compounds were successfully synthesized by structural modification of eugenol. The derivatives were spectroscopically characterized by FTIR, ^{1}H NMR, and ^{13}C NMR and prepared in good yields. Most of the derivatives used in this study demonstrated antibacterial activity against S. aureus, E. coli, K. pneumoniae, P. mirabilis, and P. aeruginosa, with zones of inhibition ranging from 11 mm to 34 mm. Among them, compound **3** showed the highest activity, which correlates with the presence of an amine group in its molecular structure. In this electrochemical study, we demonstrated that eugenol derivatives can reduce or stop the corrosion process in hydrochloric acid. Potentiodynamic polarization tests and electrochemical impedance spectroscopy revealed that the inhibitors (**2**, **3**, **3a**, **3b**, **3c**, **3d**, **3e**, **3f**) can effectively protect carbon steel against corrosion in 1.0 M HCl solution, with optimal performance at moderately higher concentrations and temperatures. Adsorption and immersion time allow the inhibitors to form a dense, stable layer on mild steel over the long term.

5. Conflicts of interest

No conflicts of interest to declare.

6. Acknowledgements

The authors would like to thank the Centre National pour la Recherche Scientifique et Technique (**CNRST**) for making the ^{1}H and ^{13}C NMR available. They would also like to express their deep gratitude to Professor **Maryse Gouygou** and **Issam Forsal** for their contribution and valuable advice in this study.

Author 1, A.B.; Author 2, C.D. Title of the article. *Abbreviated Journal Name* **Year**, *Volume*, page range.

References

1 R. R. Teixeira, P. A. R. Gazolla, A. M. Silva and M. P. G. Borsodi (2018) ***Eur. Synthesis, characterization, and biological evaluation of new heterocyclic systems 1, 2, 3-triazole-isoxazoline from eugenol by the mixed condensation reactions. J. Med. Chem.*****, 146, 274–286.**

2 S. Tazi, I. Raissouni, F. Chaoukat, D. Bouchta, A. Dahdouh, R. Elkhamlichi, and H. Douhri,(2016) Synthesis, characterization, and biological evaluation of new heterocyclic systems 1, 2, 3- triazole-isoxazoline from eugenol by the mixed condensation reactions. *J. Mater. Environ. Sci*, 7, 1642–1652.

3 B. Rebbah, A. E. Haib, S. Lahmady, I. Forsal, M. Gouygou, S.Mallet-ladeira, A. Medaghri-alaoui, E.M. Rakiba and A.Hannioui, (2024). Synthesis, characterization, and inhibition effects of a novel eugenol derivative bearing pyrrole functionalities on the corrosion of mild steel in an HCl acid solution. *RSC Adv.*, 14, 14152–14160.

4 S. S. Afridi, N. Ahmed, M. M. Zarin and M.M. Aurangzeb, (2012),. Surgical audit with risk adjusted mortality rates using the POSSUM scoring system. *J. Med. Sci.*, 25, 163–67.

5 I. Gülçin,. (2011), Antioxidant Activity of Clove Oil—A Powerful Antioxidant Source. *J. Med. Food*, 14, 975–985.

6 H.A.Buurma and B.J.Buurma, (2020,), Novel derivatives of eugenol as potent anti-inflammatory agents *via* PPARγ agonism: rational design, synthesis, analysis, PPARγ protein binding assay, and computational studies. *BMC Oral Health*, 20, 1–7.

7 S. Kotani, Y. Yoshiwara, M. Ogasawara, M. Sugiura, and M. Nakajima,(2018), Catalytic Enantioselective Aldol Reactions of Unprotected Carboxylic Acids under Phosphine Oxide Catalysis. *Angew. Chemie - Int. Ed.*, 57, 15877–15881.

8 T. Lane, M. Anantpadma, J. S. Freundlich, R. A. Davey, P. B. Madrid, and S. Ekins,(2019) The Natural Product Eugenol Is an Inhibitor of the Ebola Virus In Vitro. *Pharm. Res.*, 36, 2–7.

9 S. Sehajpal, D. N. Prasad, and R. K. Singh, (2019) *Arch. Novel ketoprofen–antioxidants mutual codrugs as safer nonsteroidal anti-inflammatory drugs: Synthesis, kinetic and pharmacological evaluation. Pharm. (Weinheim)* , 352.

10 A. T. Zari, T. A. Zari, and K. R. Hakeem, (2021) . Anticancer properties of eugenol: A review.*Molecules*, 26.

11 A. Taia*, B.El Ibrahimi, F.Benhiba, M. Ashfaq, M. Nawaz Tahir, M.Essaber, A.Aatif*,(2020) *Synth. Syntheses, single crystal X-ray structure, Hirshfeld surface analyses, DFT computations and Monte Carlo simulations of New Eugenol derivatives bearing 1,2,3-triazole moiety. Commun.* , 50, 2052–2065.

12 S. Nazreen, S. E. Elbehairi, A. M. Malebari, N. Alghamdi, R. F. Alshehri, A.A. Shati, N. M. Ali, M. Y. Alfaifi, A. A. Elhenawy, and M. M. Alam,.*(2023) New Natural Eugenol Derivatives as Antiproliferative Agents: Synthesis, Biological Evaluation, and Computational Studies. ACS Omega* , 8, 18811–18822.

13 T. Dos Santos, C. M. Coelho, T. C. Elias, F. S. Siqueira,E. S. S. Nora, M. M. A. de Campos, G. A. P. de Souza, L. F. L. Coelhob d and D. T. Carvalho,.(2019) Synthesis and biological evaluation of new eugenol-derived 1,2,3-triazoles as antimycobacterial agents. *J. Braz. Chem. Soc.* , 30, 1425–1436.

14 J. A. D. Cunha Lima, J. D. F. Silva, C. S. Santos, R. R.A. Caiana, M. M. D. Moraes, C. A.G. D. Câmara and J. C.R. Freitas. (2021) Synthesis of new 1,4-disubstituted 1,2,3-triazoles using the CuAAC reaction and determination of their antioxidant activities. ,*An. Acad. Bras. Cienc.*, , 93, 2020-1672,

15 A. Kamal, N. Shankaraiah, V. Devaiah, K. L. Reddy, A. Juvekar, S.Sen, N. Kurianb and S. Zingdeb,.(2007) Synthesis of 1,2,3-triazole-linked pyrrolobenzodiazepine conjugates employing 'click' chemistry: DNA-binding affinity and anticancer activity. *Bioorganic Med. Chem. Lett.*, 18, 1468–1473.

16 N. Upmanyu, R. Gandhi, P. Vishwavidyalaya, and K. Shah, (2011) Synthesis and anti-microbial evaluation of some novel 1 , 2 , 4 -triazole derivatives. Acta Poloniae Pharmaceutica., 68, 213-221.

17 E. Chaieb, A. Bouyanzer, B. Hammouti, and M. Benkaddour, (2005) The Inhibition Effect of Cinnamon Extract on Leaching of Aluminum Cook Wares in NaCl Solutions at Quasi-Cooking Condition. ,Journal of Surface Engineered Materials and Advanced Technology, 246, 199–206.

18 A. El Haib, A. Benharref, S. Parrès-Maynadié, E. Manoury, M. Urrutigoïty, and M. Gouygou,. (2011) Lewis acid- and Bronsted acid-catalyzed stereoselective rearrangement of epoxides derived from himachalenes: access to new chiral polycyclic structures. *Tetrahedron Asymmetry*, 22, 101–108.

19 J. El Karroumi , *A. E. Haiba, E.Manoury, A.Benharrefc,J. C. Darana, M. Gouygoua, M. Urrutigoïtya (2015), Selectivity controlled by ligand tuning in the palladium-catalysed cyclocarbonylation: Synthesis of new γ and δ lactones from a natural sesquiterpene. J. Mol. Catal. A Chem.*, 401, 18–26.

20 R. Hnini, E. Silva, L. Pinho, M. Najimi, and G. Thompson, (2023) Phenotypic Characterization and Resistance Genes Detection of Staphylococcus aureus Isolated from Bovine Mastitis in the Northwest of Portugal. *Acta Vet. Eurasia*,49, 127–136.

21 S. Lahmady, O. Anor, I. Forsal, B. Mernari, H.Hanin, K. Benbouya and A. Talfana, .(2023) Investigation of Ziziphus Lotus Leaves Extract Corrosion Inhibitory Impact on Carbon Steel in a Molar Hydrochloric Acid Solution .*Port. Electrochim. Acta.*, 41, 135–149.

22 A. Chaouiki, M. Chafiq, M. Rbaa, H.Lgaz, R.Salghi, B.Lakhrissi, I. H. Ali, S. Masroor and Y. Cho., .(2020) New 8-hydroxyquinoline-bearing quinoxaline derivatives as effective corrosion inhibitors for mild steel in HCl: Electrochemical and computational investigations. *Coatings* , 10, 811.

23 H. Boubekraoui, I. Forsal, H. Ouradi, Y. Elkhotfi, and H. Hanin, (2020) Effect of Dates Extracts as Environmentally Friendly Corrosion Inhibitor for Carbon Steel in 1M HCl Solution *Anal. Bioanal. Electrochem.* , 12, 828–840.

24 Y.El Kacimi,R.Touir, K. Alaoui, S.Kaya,A. Salem Abousalem, M. Ouakki and M. Ebn Touhami,(2020) Anti-corrosion Properties of 2-Phenyl-4(3H)-quinazolinone-Substituted Compounds: Electrochemical, Quantum Chemical, Monte Carlo, and Molecular Dynamic Simulation Investigation. *J. Bio- Tribo-Corrosion* , 6.

25 N. Errahmany, N. Errahmany, M. Rbaa, A.S. Abousalem, Ab.Tazouti, M.Galai, H. EL Kafssaoui, M. Ebn Touhami, B. Lakhrissi and R. Touir. (2020) Experimental, DFT calculations and MC simulations concept of novel quinazolinone derivatives as corrosion inhibitor for mild steel in 1.0 M HCl medium. *J. Mol. Liq* , 312 113-413, 2020.

26 M. Chafiq, A. Chaouiki, M. R. Al-Hadeethi, S. K. Mohamed ,K. Toumiat and R. Salghi,(2020) New 8-Hydroxyquinoline-Bearing Quinoxaline Derivatives as Effective Corrosion Inhibitors for Mild Steel in HCl: Electrochemical and Computational Investigations. Coatings, 10,700.

27 C. Valgas, S. M. De Souza, E. F. A. Smânia, and A. Smânia, *Brazilian.(2007) Screening methods to determine the antibacterial activity of natural products. J. Microbiol.* , 38, 369–380.